Periodic Electrolysis Technique for *In situ* Fouling Control and Removal with Low-Pressure Membrane Filtration

Hadeel Subhi Abid[a], Daniel James Johnson[a], Ben Clifford[b], David T Gethin[b], Paolo Bertoncello[a], Raed Hashaikeh[c], Nidal Hilal[a,d]*

[a]Centre for Water Advanced Technologies and Environmental Research (CWATER), College of Engineering, Swansea University, UK
[b]Welsh Centre for Printing and Coating, College of Engineering, Swansea University, UK
[c] Masdar Institute of Science and Technology, Khalifa University, Abu Dhabi, UAE
[d] College of Engineering, University of Sharjah, P. O. Box 27272 Sharjah, UAE

***Corresponding author, Email: n.hilal@swansea.ac.uk**

Submitted: December 2017

Highlights

- ►Current trend for using electrically conductive feed spacer for fouling mitigation and enhanced water flux.
- ►A study is described into humic acid removal using 2 conductive coated feed spacer configurations and their performance in a water treatment system.
- ►Effects of feed concentration, formation of bubbles during periodic electrolysis, interval time for *in situ* feed spacer cleaning and enhanced water flux were also investigated.
- ►*In situ* electrochemical cleaning through generation of bubbles is a strong advantage for using conductive feed spacer.

Abstract

Electrically conductive membranes and their application for desalination pre-treatment and water purification have an exceptional performance due to self-cleaning of fouling deposits by the application of external electric fields. However, the effectiveness of existing conductive membranes is hampered by their common applications. The current approach aims to better understand the *in situ* fouling mitigation and enhanced flux by employing two different electrically conductive coated feed spacer configurations during filtration of humic acid at concentrations of 8, 12,16 and 20 ppm. Periodic electrolysis was applied for a duration of 2 min with three intervals of 30, 45 and 60 min. A comparison of both the feed spacers was made in terms of the effect of the applied potential and interval time on enhancement of water flux, as well as the required energy consumption at four different concentrations. In terms of enhanced flux and energy consumption, feed spacer A (2×2 mm aperture size) revealed better results than feed spacer B (3×2 mm), which may be attributed to a greater conductive area. The reported technique shows a major advantage of *in situ* feed spacer self-cleaning, thus providing a continuous and non-destructive approach for the mitigation of surface fouling.

Keywords: Pre-treatment; NOM; Electrically conductive coated feed spacer; water treatment.

1. Introduction

Microfiltration is a low-pressure membrane process, which is increasingly being employed as an alternative to conventional clarification processes for the removal of microorganisms, turbidity and natural organic matter (NOM) in the water treatment process. In some situations, the microfiltration membranes are applied to obtain the ultimate treatment, while sometimes they are used as a pre-treatment for downstream advanced water treatment processes, such as reverse osmosis[1-11]. In pressure-driven membrane processes, membrane fouling is a ubiquitous phenomenon and considered to be a major problem leading to decreased flux, potentially to below the theoretical membrane capacity without appropriate treatment [8, 12-16].

Fouling is the adsorption of solute and particulates at the membrane surface or within the pores of the membrane. Mechanisms including the plugging of membrane pores, concentration polarization and cake layer formation at the membrane surface contribute to fouling build up on or within the membrane. Fouling deposits increase the required transmembrane pressure and necessitate use of chemical cleaning agents, which reduce membrane lifetime and increase operating costs [3, 17-26]. Although the fouling term can be related to both reversible and irreversible foulant adsorption, irreversible is the most problematic as it produces a flux decline that cannot be totally recovered [8, 27-31].

NOM is responsible for organic fouling and flux decline during microfiltration [32, 33]. The flux decline during water filtration results from increased resistance in the filtration system [34]. This is due to the permeability of the gel layer (surface cake) generated by colloidal material accumulation at the membrane surface, and/or to the membrane pore size reduction [18, 35-38]. Humic substances are typically classified into three categories: fulvic acids, humic acids (HA) and humin according to their solubility in water at different pH values [38, 39]. HA is an essential component of NOM and is a degradation product of biological molecules including carbohydrates, lignin, and proteins. It is commonly found in soils, and ground and surface waters in amounts varying with the seasons. It imparts a yellowish-brownish colour, as well leading to membrane fouling problems in water filtration processes [40-43]. It is a heterogeneous of both aliphatic and, aromatic components comprising three major functional groups: carboxylic acids (COOH), phenolic alcohol (OH), and methoxy carbonyl (C=O). Generally, it is more hydrophobic than other humic material. Fig.1. shows a model structure for HA [44].

Nanofiltration and reverse osmosis processes have been broadly used to remove humic substances, since they have many advantages, such as small footprint area, high product quality, and lowered chemical reagent use. However, these membranes operate at high-pressure, which leads to high water costs [17, 45-50], as humic substance adsorption at the membrane surface results in increased hydraulic pressure requirements and operating efficiency losses. Therefore, pre-removal of humic substances using low-pressure membranes is an active area of research [50, 51].

Fouling models for microfiltration are used to determine the optimal set of operating conditions that minimize fouling and the frequency of backwashing and/or chemical cleaning required [31]. Previous investigations have sought to remove HA from feed water, assuming that HA is the major foulant type [29]. Yuan *et al.* [38] investigated filtration of 2 mg/l HA solutions through a 0.22 μm poly(vinylidene fluoride)PVDF microfiltration membrane for durations of 1, 5, 20 and 100 min. The initial filtration value for the membrane was 1.010 $x10^{-3}$ m/s. The authors stated that the relative flux declined to less than 10% of its initial value within the initial 20 min at a constant pressure 0.69 bar. The data obtained demonstrated that HA fouling during microfiltration is dominated by the convective deposition of a fouling component at the membrane upper surface. A model was also developed to describe the water flux behaviour as a function of time for a wide range of conditions. Lin *et al*.[11] studied fouling of PVDF microfiltration membranes whilst filtering HA suspensions with concentrations of 2 and 4 ppm for 100 min operation time. Ultrasound signals were used to study fouling deposition at different time intervals. They recommended that it is essential to design a proper filtration module allowing *in situ* cleaning of the membrane to mitigate fouling.

Applied electric force is a powerful means to decrease the membrane fouling caused by negatively charged organic pollutants, is an environmentally benign technique, with significant milestones achieved commercially and scientifically so far [26]. This method is sometimes known as electro-filtration [52]. In an electrochemical water treatment set-up, the conductive substrate performs as the anode, causing direct oxidation of foulants [53], or as a cathode, where foulants are removed via generation of tiny bubbles at the conductive surface [54]. This is the principal mechanism on which electrochemical membrane fouling mitigation is based [52]. However, it has recently been suggested that whilst bubble formation via electro-reduction is an efficient mechanism for *in situ* cleaning of membranes, the oxidation method may damage the membrane itself [55-59]. Bubbles offer a promising option for a

clean, inexpensive and environmentally friendly technique appropriate for *in situ* cleaning of conducting substrates. However, the use of the bubbles in new technology is yet to be investigated and is challenging to implement [60].

When modifying membranes several studies have found that the thin coatings are eroded due to water flow. As a result, much attention has turned to examination of modification of feed spacers, which can have thicker and more durable coatings applied without affecting membrane transport [59]. As a result, several studies have highlighted the use of an electrically conductive feed spacer to prevent biological and organic fouling. Noticeable flux recovery was detected, which was related to the electrostatic repulsion between the foulant and the feed spacer strand [59]. Baek *et al*.[61] employed a lab scale cross-flow system with a titanium feed spacer. The feed spacer was activated via application of positive, negative and alternating potential for 30 min to de-foul *P. aeruginosa PA01 GFP* biofilm layers. Consequently, permeate flux recovery was achieved. In our previous study [55] we investigated the ability of the application of an electrically conductive feed spacer to function as a means for limiting organic fouling in a lab scale cross-flow system. An aqueous suspension of 20 ppm sodium alginate was employed (as model organic foulant), which acted as the electrolyte solution. When an electrical potential was applied, *in situ* fouling mitigation was observed with noticeable flux enhancement without any obvious damage to the membrane surface.

The objective of the current research was to study the effects of applied periodic electrolysis on water flux and flux recovery after fouling, through a combined use of electrically conductive feed spacer with microfiltration membranes. These investigations were performed with HA filtration at concentrations of 8, 12, 16 and 20 ppm for three intervals of 30, 45 and 60 min duration, employing two configurations of feed spacers.

2. Materials and Methods

2.1 Materials

Polypropylene feed spacer with two different configuration, mesh A with aperture size 2×2 mm (diamond shape) and mesh B with aperture size 3×3 mm (GE, USA) were employed as a feed spacer in the filtration system; both of the meshes were coated with a carbon-based ink comprised of graphene nanoplates (GNPs) using a dipped coating method, which has been reported elsewhere [55]. PVDF membranes (Millipore, pore size 0.22 mm: See table 2), sodium chloride, HA (HA), sodium dodecylbenzene sulfonate (SDBS) and a 0.45 μm cellulose acetate membranes were purchased from Sigma Aldrich (Dorset, UK).

2.2. Experimental Method

HA powder (1g) was dissolved in 1000 ml deionized water (MilliQ). Solution pH was measured using a Jenway pH meter model 3540. The pH values of the solutions were adjusted to pH 10 by adding 0.1 M NaOH, before filtration through a 0.45 μm cellulose acetate filter membrane to remove all suspended solids, and stored at 4.5°C. The feed solutions of HA at concentrations of 8, 12, 16 and 20 ppm were prepared for all experiments using deionized water and adjusted to pH 7.0 by addition of 0.1 M NaOH or HCl as needed. Sodium chloride was added to a final concentration of 10,000 ppm to assist the electrolysis process during *in situ* substrate cleaning. The filtration process was carried out using two configurations of feed spacer (A and B) at room temperature (22 ^{o}C ±1) with constant pressure of 0.5 bar and a flow rate of 0.58 ± 0.01 L.min^{-1}. Electrical potential was applied for 2 min with intervals of different duration: 30min (6 cleaning cycles), 45 min (4 cycles) and 60 min (3 cycles), then the permeation flux was calculated.

For electrolytic cleaning, a polycarbonate cross-flow cell was employed. The coated feed spacer combined with commercial membrane acted as a cathode and the graphite electrode (diameter 15 mm) as an anode in electrochemical system. A graphite electrode was selected because it is electrically neutral and does not dissolve in water under the effect of current [55, 62]. Experiments were performed in a lab-scale apparatus (Fig 2), using a CHI-760E potentiostat at - 6 V for 2 min. The orientation of feed spacer versus the bulk flow direction (channel axis) is shown in Fig 3. The performance of two types configuration for improved water flux were investigated during 200min filtration time.

2.3 Characterization

2.3.1 Electrochemical Analysis (CV and LSV)

Linear sweep voltammetry (LSV) and Cyclic voltammetry (CV) were performed in an analytical model CHI-760E potentiostat (CH Instruments, Inc., USA). A conventional three-electrode assembly consisting of a Pt wire counter electrode and an Ag/AgCl (3.5 M KCl) reference electrode were used for the electrochemical measurements of the both conductive feed spacers (A and B), which performed as a working electrode. In these experiments, all the potentials were recorded versus the Ag/AgCl reference electrode, in acidic solution (0.5 M H_2SO_4). The adopted scanning rate was 0.05 V/s.

2.3.2 Morphology

The morphology characterization of the coating feed spacer and the durability for the both feed spacers were observed using FE-SEM imaging (Hitachi-S4800). For each sample, areas of 1 cm^2 were cut and used, also the morphology of coating prior and after applied potential and were examined.

2.3.3 Zeta potential measurement

A universal capillary cuvette cell (DTS 1070), as an accessary for Zetasizer (Malvern Instruments, UK), was employed to determine the zeta-potential of fouling solution prior to use [63]. A dip cell kit (ZEN1002) was employed to measure the surface zeta-potential for the membrane surface [64]. All measurement was done at PH 7, using 0.1 M NaOH and 0.1 M HCl to titrate PH to 7.

2.3.4. Pure water flux and peat water flux

Pure water flux (PWF) was measured using DIW in cross flow set-up at constant pressure 0.5 bar and a flow rate 0.58 ± 0.01 $L.min^{-1}$, PWF and peat water flux was calculated by the following equation [50]:.

$$Jw = \frac{V}{A\,\Delta t} \qquad (1)$$

Where J_w is the water flux, V is the volume of filtrate water collected, Δt is the water filtration time and A is the active area in the electrochemical cell.

3. Results and Discussion

The coatings of the surface feed spacers were characterized by SEM imaging, with representative images shown in Fig. 4-a and Fig. 4-b. The durability of the surface coating prior to and after applied potential, was observed, as shown in Fig. 4-c and Fig. 4-d, with the overall structures of the before and after surface appearing similar. As such, no apparent damage to the structure of the feed spacer surface coating due to the applied potential was identified.

The electrochemical behaviour of the feed spacers was investigated using both linear sweep and cyclic voltammetry methods. Fig 5 & Fig 6 show a comparison of both feed spacer A and feed spacer B with the commercial titanium mesh (as a reference for the conductivity activity of the coated feed spacer). It can be seen that hydrogen bubble evolution on feed spacer A started at -0.79V and at -0.81 V for feed spacer B (vs Ag/AgCl reference) compared with the titanium metal mesh, where it began at -0.5V. Accordingly, the results reveal that there is a need for applying overpotential for both feed spacer A and B compared with the reference mesh.

Zeta potential measurements were used to evaluate the charge of the feed solution at 8, 12, 16 and 20 ppm and surface charge of membrane at pH 7.0. The feed solution was found to be negatively charged at -27.7 mV (at concentration 8 ppm), -30.3 mV (12 ppm), -32.9 mV (16 ppm) and -40.3 mV (20 ppm) (table 1). Consequently, that will be a helpful parameter to increase the repulsion force and enhance the *in situ* surface cleaning during applied potential through the feed spacer.

3.1 Investigation of the impact of applied potential on fouling and the water flux

The *in situ* cleaning performance of the electrically conductive coated feed spacers combined with PVDF membrane was evaluated by HA solution filtration processes. During the electrolysis process at the cathodic feed spacer / electrolyte interface, bubbles are generated at the surface of the feed spacer and begin moving up and then depart after achieving an appropriate size. The long stay of bubbles on the feed spacer surface reduces the ion transfer reaction and consequently reduces the efficiency of the electrolysis process (appropriate applied voltage should be considered). HA solutions were filtered at a pressure of 0.5 bar with flux recorded as a function of time. The self-cleaning method was applied (at -6 V potential for 2 min) in the presence of either feed spacer A or B for different concentrations

of feed solution and different intervals time for each concentration. As shown in Figures 7 to 10., there is an obvious decline in water flux at 8ppm, 12 ppm ,16 ppm and 20 ppm concentrations. The *in situ* de-fouling behaviour for the two configurations feed spacer at the four different concentrations was studied and evaluated at constant pressure and flow rate.

3.1 1 Feed spacer A results

Feed spacer A was used to test and compare the permeate flux with and without the presence of periodic electrolysis after 200 min water-filtration time. A clear decline in water flux was seen at HA concentrations of 8ppm (See: Fig. 7-a, Fig.7-c and Fig.7-e), 12 ppm (See: Fig. 8-a, Fig.8-c and Fig.8-e), 16 ppm (See: Fig. 9-a, Fig.9-c and Fig.9-e), and at 20 ppm (See: Fig.10-a, Fig.10-c and Fig.10-e).

During the self-cleaning process (Fig. 7-a), 8 ppm foulant solution of HA was filtered for 30min leading to a decline in relative water flux to 0.339. When the first electrolysis *in situ* cleaning was applied for 2 min recovery in relative flux to 0.977 was obtained. After another 30-min filtration period the relative flux significantly declined to 0.156 and again was recovered to 0.875 after the second cleaning and increased from 0.104 to 0.748 after the third cleaning. After the fourth interval filtration time (after 120min) the relative flux reached 0.089, with further 2min application of electrolysis leading to relative flux recovery at 0.563, while at 150min filtration-time the relative flux decreased to 0.069, which improved to 0. 379. Finally, the relative flux was raised from 0.065 to 0.270 due to self-cleaning by running electrolysis for 2min at 180min.

The flux recovery investigations for feed spacer A were also performed after 45min and 60 min intervals time as shown in Fig. 7-b and Fig7-c. Relative flux improvement from 0.226 to 0.938 can be seen after 45 min filtration time when the first self-cleaning was performed for 2min. Meanwhile the considerable improvement in relative flux from 0.093 to 0.751 after the second cleaning was achieved. It also improved from 0.059 to 0.458 after the third *in situ* cleaning and from 0.0527 to 0.267 after the fourth 2 min application of periodic electrolysis. A subsequent improvement in relative flux from 0.137 to 0.853, from 0.067 to 0.532 and from 0.054 to 0.249 were obtained after three intervals (60min ,120min and 180min respectively). The consequence of filtration cycle time on the water flux recovery was acted via electrolysis cleaning after 30, 45 and 60 min respectively for feed spacer configuration A at 12ppm (See: Fig 8-a, Fig 8-c and Fig 8-e), 16ppm (See: Fig 9-a, Fig 9-c and Fig 9-e) and 20ppm (See: Fig 10-a, Fig 10-c and Fig 10-e) respectively. As would be expected, flux

decline between cleaning cycles was most pronounced for longer interval durations, with little difference seen between different concentrations of foulant.

3.1 2 Feed spacer B results

The same behaviour was observed when employing electrically conductive coated feed spacer B for the same interval times. For *in situ* cleaning at 8 ppm HA concentration the flux declined to 0.323, with the first *in situ* cleaning performed for 2 min leading to an improvement in relative flux to 0.968 (Fig. 7-b). After the 2nd filtration period (60 min) the relative flux noticeably decreased to 0.155 and again was increased to 0.866. after the third *in situ* cleaning, it was enhanced from 0.099 to 0.631. After 120min filtration time (fourth interval), the relative flux reached 0.085, with the application of electrolysis for 2min, an increase in relative flux to 0.411. At 150 min filtration time the relative flux declined to 0.066, which recovered to 0. 271. Eventually, the relative flux improved from 0.062 to 0.193 due to 2min running electrolysis at 180min filtration time. The flux recovery was also studied for four filtration intervals between cleaning applications (each 45min) and three intervals (each 60 min) as shown in Fig. 7-d and Fig7-f. Relative flux enhancement from 0.156 to 0.902 was seen for the first self-cleaning cycle (after 45 min filtration time), reduced to 0.127 to 0.592 after the second self-cleaning cycle was applied. It also increased from 0.078 to 0.371 after the third cleaning and from 0.064 to 0.106 at the fourth application of periodic electrolysis. A consequent progress in relative flux from 0.088 to 0.737, from 0.058 to 0.374 and from 0.049 to 0.097 were obtained after three cleaning cycles (i.e. after each 60min). The consequence of filtration cycle-time on the water-flux recovery was also observed after 30, 45 or 60 min for feed spacer configuration B at 12ppm (See: Fig 8-b, Fig 8-d and Fig 8-f), 16ppm (See: Fig 9-b, Fig 9-d and Fig 9-f) and 20ppm (See: Fig 10-b, Fig 10-d and Fig 10-f) respectively.

For both feed spacers, the same inclination was observed when employing feed spacer for the same interval time. The relative flux over a 200-min test-period is shown in Fig.7, Fig.8, Fig.9 and Fig.10 respectively, where all the results due to applied potential performed better than without applied potential. The significantly higher recovery of relative flux was shown during applied potential (2min) for different interval time at the same test-period. However, feed spacer A optional is showed better performance than for feed space B in terms of enhanced flux and water flow.

3.2 An Investigation of the impact of number of cleaning applications on the final flux

Number of electrolysis applications during filtration processes played a vital role in water flux and permeate flux production. For both feed spacers A and B, a comparison of filtration interval duration: 30 min, 45 min and 120 min versus the relative flux was investigated. Each feed spacer configuration and fouling concentration showed a significant enhancement in relative flux recovery when a greater number of cleaning cycles, and hence shorter filtration times, were used. As shown in Fig.11, Fig.12, Fig.13 and Fig.14, The higher number of cleaning cycles,, the higher the permeate flux for a certain HA concentration. However, in case of applied feed spacer A, a better relative flux recovery was observed due to a greater electrically conductive area, despite having a smaller mesh opening area compared with feed spacer B.

3.3. Energy consumption aspects

Economic analysis is essential to scale the application of modified feed spacer from laboratory observations to pilot or industrial scale. The energy consumption was investigated based upon the amount of electrical energy consumed in kWh by the pump, which was employed for re-circulating feed as well as due to the electrical potential applied for electrolysis. The effect of applied potential for 2 min on the energy consumption was also explored during *in situ* cleaning for 3, 4, and 6 cleaning cycles. For feed spacer A, 0.001 kwh was required for applied potential V for 2 min. Meanwhile for feed spacer B the energy demand was 0.002 kWh to apply the same potential and for the same duration. In addition, the pumping system consumed 0.013 kWh for 200 min operation filtration time, which was identical for both feed spacer configurations.

The overall consumption energy (including the energy required to re-circulating feed added to the energy required to applied potential during in situ cleaning) versus permeate flux production ratio for feed spacer A was 0.019 kWh (6 applications),0.017 kWh (4 applications) and 0.016 kWh (3 applications), while it was 0.025 kWh (6 applications), 0.021 (4 applications) and 0.019 (3 applications) for feed spacer B. The specific energy consumption versus the number of intervals is shown in Fig. 15. Feed spacer A shows a better relative flux enhancement, it also required half the energy to maintain the same electrical potential as B, demonstrating superior performance (See Fig 16).

4. Conclusion

In this study, an *in situ* cleaning method using periodic electrolysis was investigated for two configurations electrically conductive coated feed spacers. An obvious improvement in water flux recovery was seen due to this cleaning process. The *in situ* membrane cleaning effect was evaluated by filtration of a HA suspension. The self-cleaning process was carried out in electrochemical cross-flow set-up. Applying periodic electrolysis lead to the formation of tiny bubbles on the feed spacer filaments, which play a vital role in release of fouling deposits from the membrane and spacer elements. The main advantage of this technique is that it can be employed directly to a membrane module between filtration intervals without the need for backwashing or application of caustic chemicals. This method for cleaning membrane is promising for membranes processes where flux reduction and fouling pose an essential issue. However, much work is still needed for developing improved feed spacer as well as to study the underlying membrane performance in term of selectivity and permeability in future.

Nomenclatures

NOM	Natural organic matter
HA	Humic acid
PVDF	Poly(vinylidene fluoride)
COOH	Carboxylic acids
OH	Phenolic alcohol
C=O	Methoxy carbonyl
SDBS	Sodium dodecylbenzene sulfonate
HCl	Hydrochloride acid
NaOH	Sodium hydroxide
DIW	Deionized water
LSV	Linear sweep voltammetry
CV	Cyclic voltammetry
KCl	Potassium chloride
SEM	Scanning electron microscope
Zp	Zeta potential

References:

[1] B. Malczewska, J. Liu, M.M. Benjamin, Virtual elimination of MF and UF fouling by adsorptive pre-coat filtration, Journal of Membrane Science, 479 (2015) 159-164.
[2] K. Katsoufidou, S.G. Yiantsios, A.J. Karabelas, An experimental study of UF membrane fouling by humic acid and sodium alginate solutions: the effect of backwashing on flux recovery, Desalination, 220 (2008) 214-227.
[3] C. Güell, P. Czekaj, R.H. Davis, Microfiltration of protein mixtures and the effects of yeast on membrane fouling, Journal of Membrane Science, 155 (1999) 113-122.
[4] T. Carroll, S. King, S.R. Gray, B.A. Bolto, N.A. Booker, The fouling of microfiltration membranes by NOM after coagulation treatment, Water Research, 34 (2000) 2861-2868.
[5] V.T. Kuberkar, R.H. Davis, Effects of Added Yeast on Protein Transmission and Flux in Cross-Flow Membrane Microfiltration, Biotechnology Progress, 15 (1999) 472-479.
[6] W. Yuan, A.L. Zydney, Effects of solution environment on humic acid fouling during microfiltration, Desalination, 122 (1999) 63-76.
[7] W. Yuan, A.L. Zydney, Humic acid fouling during microfiltration, Journal of Membrane Science, 157 (1999) 1-12.
[8] K.L. Jones, C.R. O′Melia, Protein and humic acid adsorption onto hydrophilic membrane surfaces: effects of pH and ionic strength, Journal of Membrane Science, 165 (2000) 31-46.
[9] S.R. Holman, K.N. Ohlinger, An Evaluation of Fouling Potential and Methods to Control Fouling in Microfiltration Membranes for Secondary Wastewater Effluent, Proceedings of the Water Environment Federation, 2007 (2007) 6417-6444.
[10] H. Huang, T.A. Young, J.G. Jacangelo, Unified Membrane Fouling Index for Low Pressure Membrane Filtration of Natural Waters: Principles and Methodology, Environmental Science & Technology, 42 (2008) 714-720.
[11] Y.-H. Lin, K.-L. Tung, S.-H. Wang, Q. Zhou, K.K. Shung, Distribution and deposition of organic fouling on the microfiltration membrane evaluated by high-frequency ultrasound, Journal of Membrane Science, 433 (2013) 100-111.
[12] R.W. Field, D. Wu, J.A. Howell, B.B. Gupta, Critical flux concept for microfiltration fouling, Journal of Membrane Science, 100 (1995) 259-272.
[13] D. Johnson, F. Galiano, S.A. Deowan, J. Hoinkis, A. Figoli, N. Hilal, Adhesion forces between humic acid functionalized colloidal probes and polymer membranes to assess fouling potential, Journal of Membrane Science, 484 (2015) 35-46.
[14] W.J.T. Lewis, A. Agg, A. Clarke, T. Mattsson, Y.M.J. Chew, M.R. Bird, Development of an automated, advanced fluid dynamic gauge for cake fouling studies in cross-flow filtrations, Sensors and Actuators A: Physical, 238 (2016) 282-296.
[15] A. Sagiv, R. Semiat, Backwash of RO spiral wound membranes, Desalination, 179 (2005) 1-9.
[16] S. Zou, Y.-N. Wang, F. Wicaksana, T. Aung, P.C.Y. Wong, A.G. Fane, C.Y. Tang, Direct microscopic observation of forward osmosis membrane fouling by microalgae: Critical flux and the role of operational conditions, Journal of Membrane Science, 436 (2013) 174-185.
[17] X. Cui, K.-H. Choo, Natural Organic Matter Removal and Fouling Control in Low-Pressure Membrane Filtration for Water Treatment, Environmental Engineering Research, 19 (2014) 1-8.
[18] N. Lee, G. Amy, J. Lozier, Understanding natural organic matter fouling in low-pressure membrane filtration, Desalination, 178 (2005) 85-93.
[19] K. Boussu, A. Belpaire, A. Volodin, C. Van Haesendonck, P. Van der Meeren, C. Vandecasteele, B. Van der Bruggen, Influence of membrane and colloid characteristics on fouling of nanofiltration membranes, Journal of Membrane Science, 289 (2007) 220-230.
[20] L.Y. Ng, A.W. Mohammad, C.P. Leo, N. Hilal, Polymeric membranes incorporated with metal/metal oxide nanoparticles: A comprehensive review, Desalination, 308 (2013) 15-33.

[21] J.A. Reverter, S. Talo, J. Alday, Las Palmas III — the success story of brine staging, Desalination, 138 (2001) 207-217.
[22] T. Nguyen, F. Roddick, L. Fan, Biofouling of Water Treatment Membranes: A Review of the Underlying Causes, Monitoring Techniques and Control Measures, Membranes, 2 (2012) 804.
[23] T.J. Ainscough, D.L. Oatley-Radcliffe, A.R. Barron, Parametric optimisation for the fabrication of polyetherimide-sPEEK asymmetric membranes on a non-woven support layer, Separation and Purification Technology, 186 (2017) 78-89.
[24] K. Xiao, X. Wang, X. Huang, T.D. Waite, X. Wen, Analysis of polysaccharide, protein and humic acid retention by microfiltration membranes using Thomas′ dynamic adsorption model, Journal of Membrane Science, 342 (2009) 22-34.
[25] Y. Sun, Z. Qin, L. Zhao, Q. Chen, Q. Hou, H. Lin, L. Jiang, J. Liu, Z. Du, Membrane fouling mechanisms and permeate flux decline model in soy sauce microfiltration, Journal of Food Process Engineering, e12599-n/a.
[26] X. Li, Y. Mo, J. Li, W. Guo, H.H. Ngo, In-situ monitoring techniques for membrane fouling and local filtration characteristics in hollow fiber membrane processes: A critical review, Journal of Membrane Science, 528 (2017) 187-200.
[27] H. Lin, M. Zhang, F. Wang, F. Meng, B.-Q. Liao, H. Hong, J. Chen, W. Gao, A critical review of extracellular polymeric substances (EPSs) in membrane bioreactors: Characteristics, roles in membrane fouling and control strategies, Journal of Membrane Science, 460 (2014) 110-125.
[28] W. Yu, N.J.D. Graham, Performance of an integrated granular media − Ultrafiltration membrane process for drinking water treatment, Journal of Membrane Science, 492 (2015) 164-172.
[29] Q. She, R. Wang, A.G. Fane, C.Y. Tang, Membrane fouling in osmotically driven membrane processes: A review, Journal of Membrane Science, 499 (2016) 201-233.
[30] G. Amy, Fundamental understanding of organic matter fouling of membranes, Desalination, 231 (2008) 44-51.
[31] J. Kim, F.A. DiGiano, Fouling models for low-pressure membrane systems, Separation and Purification Technology, 68 (2009) 293-304.
[32] H. Yamamura, K. Okimoto, K. Kimura, Y. Watanabe, Hydrophilic fraction of natural organic matter causing irreversible fouling of microfiltration and ultrafiltration membranes, Water Research, 54 (2014) 123-136.
[33] K. Jeong, D.G. Kim, S.O. Ko, Adsorption characteristics of Effluent Organic Matter and Natural Organic Matter by Carbon Based Nanomaterials, KSCE Journal of Civil Engineering, 21 (2017) 119-126.
[34] D. Rana, T. Matsuura, Surface Modifications for Antifouling Membranes, Chemical Reviews, 110 (2010) 2448-2471.
[35] L. Fan, J.L. Harris, F.A. Roddick, N.A. Booker, Influence of the characteristics of natural organic matter on the fouling of microfiltration membranes, Water Research, 35 (2001) 4455-4463.
[36] K. Katsoufidou, S.G. Yiantsios, A.J. Karabelas, An experimental study of UF membrane fouling by humic acid and sodium alginate solutions: the effect of backwashing on flux recovery, Desalination, 220 (2008) 214-227.
[37] R. Shang, H.p. Deng, J.y. Hu, Removal of humic acid by a new type of electrical hollow-fiber microfiltration (E-HFMF), AIP Conference Proceedings, 1251 (2010) 97-100.

[38] W. Yuan, A. Kocic, A.L. Zydney, Analysis of humic acid fouling during microfiltration using a pore blockage–cake filtration model, Journal of Membrane Science, 198 (2002) 51-62.
[39] H. Fakour, T.-F. Lin, Effect of Humic Acid on As Redox Transformation and Kinetic Adsorption onto Iron Oxide Based Adsorbent (IBA), International Journal of Environmental Research and Public Health, 11 (2014) 10710.
[40] Y. Wei, H. Chu, B. Dong, X. Li, Evaluation of humic acid removal by a flat submerged membrane photoreactor, Chinese Science Bulletin, 56 (2011) 3437-3444.
[41] M. Nyström, K. Ruohomäki, L. Kaipia, Humic acid as a fouling agent in filtration, Desalination, 106 (1996) 79-87.
[42] M.N. Abu Seman, N. Hilal, M. Khayet, UV-photografting modification of NF membrane surface for NOM wfouling reduction, Desalination and Water Treatment, 51 (2013) 4855-4861.
[43] B. Malczewska, J. Liu, M.M. Benjamin, Virtual elimination of MF and UF fouling by adsorptive pre-coat filtration, Journal of Membrane Science, 479 (2015) 159-164.
[44] A.W. Zularisam, A.F. Ismail, R. Salim, Behaviours of natural organic matter in membrane filtration for surface water treatment — a review, Desalination, 194 (2006) 211-231.
[45] D.J. Johnson, W.A. Suwaileh, A.W. Mohammed, N. Hilal, Osmotic's potential: An overview of draw solutes for forward osmosis, Desalination, (2017).
[46] D.L. Oatley-Radcliffe, M. Walters, T.J. Ainscough, P.M. Williams, A.W. Mohammad, N. Hilal, Nanofiltration membranes and processes: A review of research trends over the past decade, Journal of Water Process Engineering, 19 (2017) 164-171.
[47] K. Wang, A.A. Abdalla, M.A. Khaleel, N. Hilal, M.K. Khraisheh, Mechanical properties of water desalination and wastewater treatment membranes, Desalination, 401 (2017) 190-205.
[48] P.S. Goh, T. Matsuura, A.F. Ismail, N. Hilal, Recent trends in membranes and membrane processes for desalination, Desalination, 391 (2016) 43-60.
[49] W.L. Ang, A.W. Mohammad, Y.H. Teow, A. Benamor, N. Hilal, Hybrid chitosan/FeCl3 coagulation–membrane processes: Performance evaluation and membrane fouling study in removing natural organic matter, Separation and Purification Technology, 152 (2015) 23-31.
[50] P.T.P. Aryanti, S. Subagjo, D. Ariono, I.G. Wenten, Fouling and Rejection Characteristic of Humic Substances in Polysulfone Ultrafiltration Membrane, Journal of Membrane Science and Research, 1 (2015) 41-45.
[51] A. Charfi, H. Jang, J. Kim, Membrane fouling by sodium alginate in high salinity conditions to simulate biofouling during seawater desalination, Bioresource Technology, 240 (2017) 106-114.
[52] X. Shi, G. Tal, N.P. Hankins, V. Gitis, Fouling and cleaning of ultrafiltration membranes: A review, Journal of Water Process Engineering, 1 (2014) 121-138.
[53] C.-F. de Lannoy, D. Jassby, K. Gloe, A.D. Gordon, M.R. Wiesner, Aquatic Biofouling Prevention by Electrically Charged Nanocomposite Polymer Thin Film Membranes, Environmental Science & Technology, 47 (2013) 2760-2768.
[54] Z. Wu, H. Chen, Y. Dong, H. Mao, J. Sun, S. Chen, V.S.J. Craig, J. Hu, Cleaning using nanobubbles: Defouling by electrochemical generation of bubbles, Journal of Colloid and Interface Science, 328 (2008) 10-14.
[55] H.S. Abid, B.S. Lalia, P. Bertoncello, R. Hashaikeh, B. Clifford, D.T. Gethin, N. Hilal, Electrically conductive spacers for self-cleaning membrane surfaces via periodic electrolysis, Desalination, 416 (2017) 16-23.

[56] F. Ahmed, B.S. Lalia, V. Kochkodan, N. Hilal, R. Hashaikeh, Electrically conductive polymeric membranes for fouling prevention and detection: A review, Desalination, 391 (2016) 1-15.
[57] R. Hashaikeh, B.S. Lalia, V. Kochkodan, N. Hilal, A novel in situ membrane cleaning method using periodic electrolysis, Journal of Membrane Science, 471 (2014) 149-154.
[58] B.S. Lalia, F.E. Ahmed, T. Shah, N. Hilal, R. Hashaikeh, Electrically conductive membranes based on carbon nanostructures for self-cleaning of biofouling, Desalination, 360 (2015) 8-12.
[59] H.S. Abid, D.J. Johnson, R. Hashaikeh, N. Hilal, A review of efforts to reduce membrane fouling by control of feed spacer characteristics, Desalination, 420 (2017) 384-402.
[60] A. Agarwal, W.J. Ng, Y. Liu, Principle and applications of microbubble and nanobubble technology for water treatment, Chemosphere, 84 (2011) 1175-1180.
[61] Y. Baek, H. Yoon, S. Shim, J. Choi, J. Yoon, Electroconductive Feed Spacer as a Tool for Biofouling Control in a Membrane System for Water Treatment, Environmental Science & Technology Letters, 1 (2014) 179-184.
[62] N. Bidin, S.R. Azni, S. Islam, M. Abdullah, M.F.S. Ahmad, G. Krishnan, A.R. Johari, M.A.A. Bakar, N.S. Sahidan, N. Musa, M.F. Salebi, N. Razali, M.M. Sanagi, The effect of magnetic and optic field in water electrolysis, International Journal of Hydrogen Energy, 42 (2017) 16325-16332.
[63] M. Martínez-Carmona, D. Lozano, M. Colilla, M. Vallet-Regí, Lectin-conjugated pH-responsive mesoporous silica nanoparticles for targeted bone cancer treatment, Acta Biomaterialia, 65 (2018) 393-404.
[64] T.E. Thomas, S.A. Aani, D.L. Oatley-Radcliffe, P.M. Williams, N. Hilal, Laser Doppler Electrophoresis and electro-osmotic flow mapping: A novel methodology for the determination of membrane surface zeta potential, Journal of Membrane Science, 523 (2017) 524-532.

List of Figures

Fig: 14: A comparison between relative flux values of HA with concentration 20 ppm gained after each interval for using both feed spacer A and feed spacer B (a) 30min interval filtration (b) 45min interval filtration (c) 60min interval filtration.

Fig 15: The specific consumption energy for (a) 8, (b) 12, (c) 16 and (d) 20 ppm humic acid concentration during 6, 4, 3 and zero intervals applied potential time for Feed Spacer A and B.

Fig: 16: The effect of feed spacer configuration on the consumption energy.

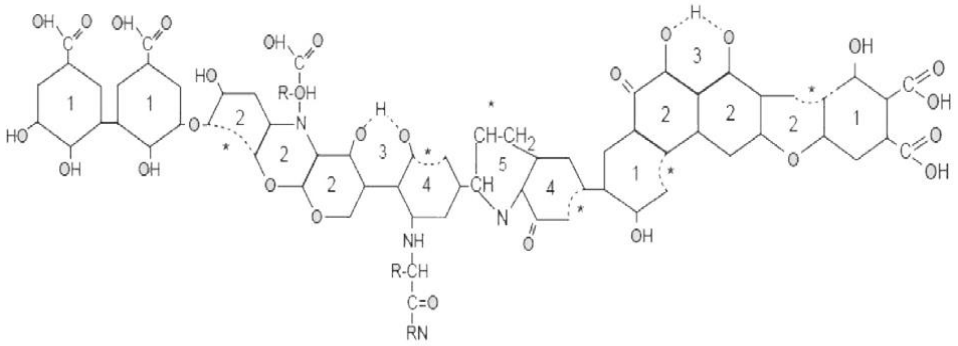

Fig: 1: Model structure of Humic Acid[44]

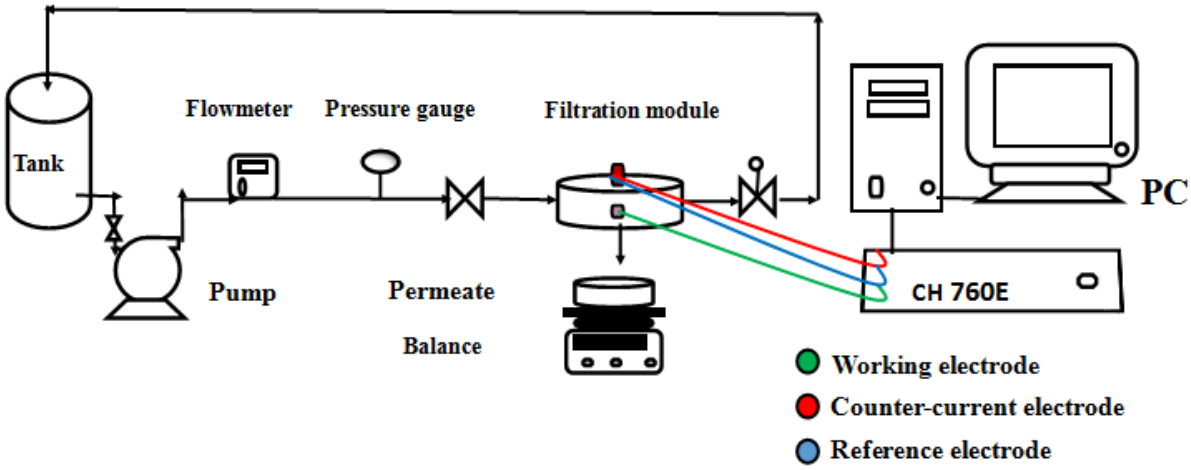

Fig: 2: Schematic representation of the enhanced cross-flow set-up

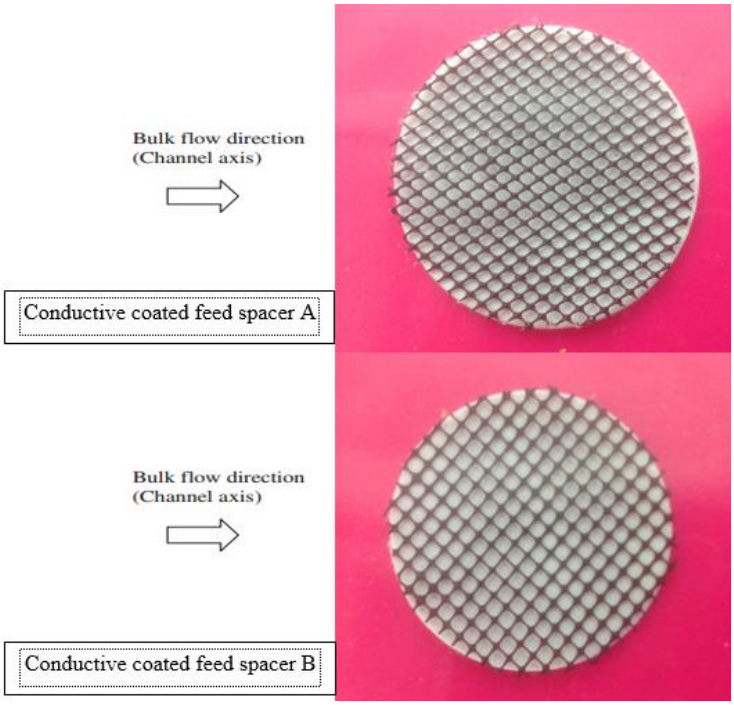

Fig: 3: Top view of feed spacer orientation combined with PVDF microfiltration versus bulk flow direction for conductive coated feed spacer A with aperture size 2×2 mm diamond shape and conductive coated feed spacer B with aperture size 3×3 mm.

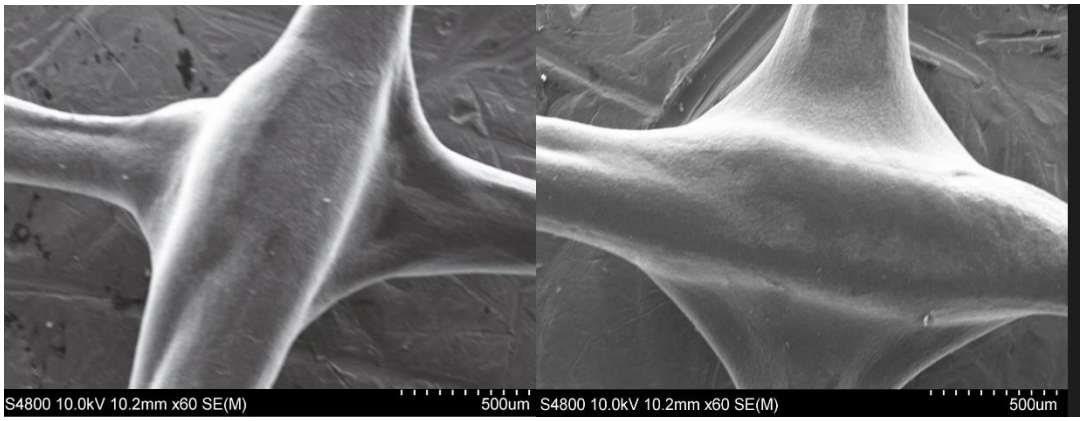

(A) **(B)**

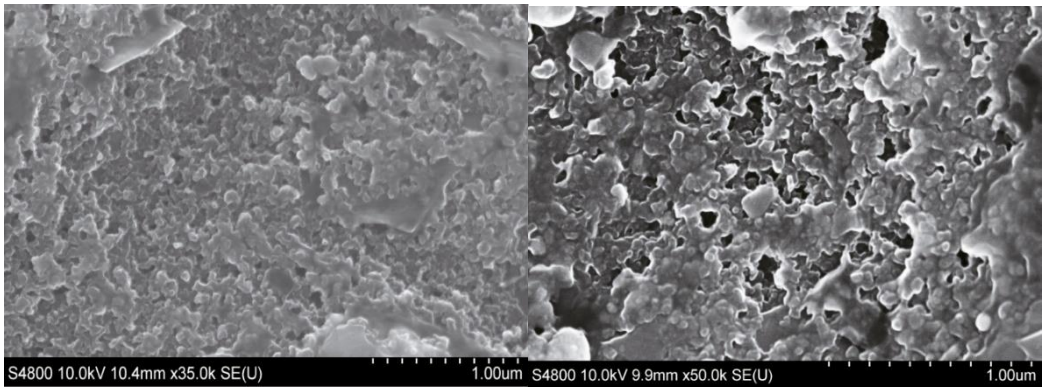

(C) **(D)**

Fig: 4: a) The surface morphology of the coating of feed spacer A b) The surface morphology of the coating of feed spacer B c) the morphology of coating prior to applied potential d) the morphology of coating after applied potential.

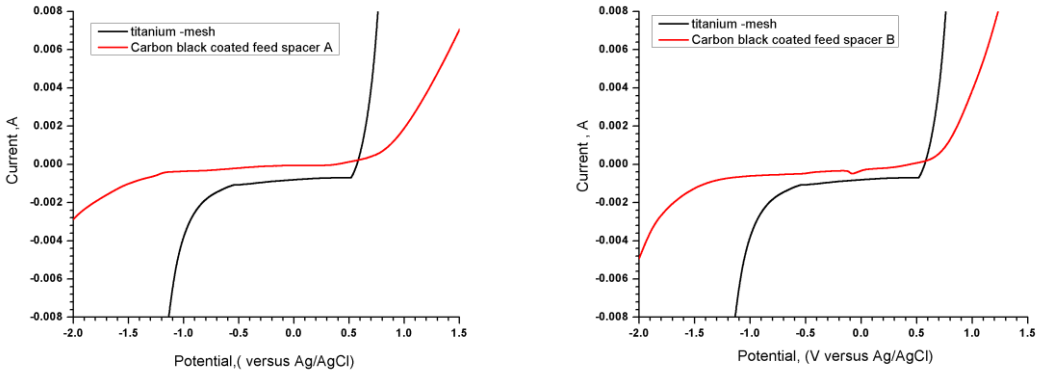

A **B**

Fig: 5: Linear sweep voltammetry(LSV) of electrically conductive feed spacer and titanium metal mesh (a) feed spacer A (b) feed spacer B.

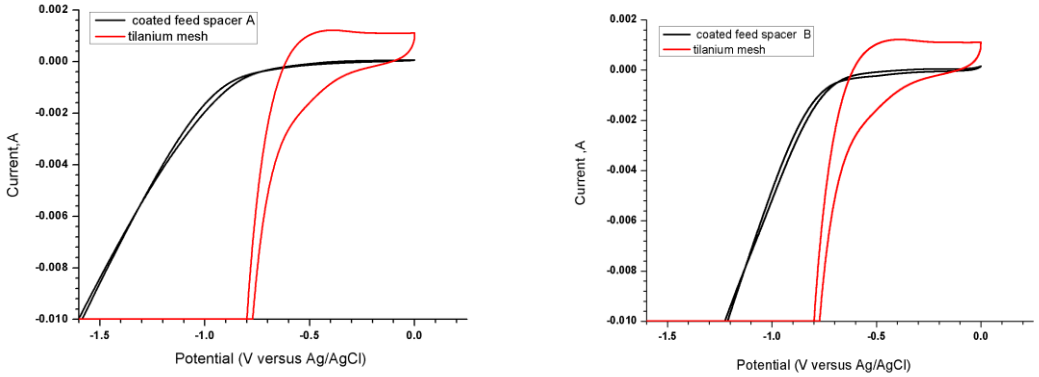

Fig: 6: Cyclic voltammetry(CV) of electrically conductive feed spacer and titanium metal mesh (a) feed spacer A (b) feed spacer B.

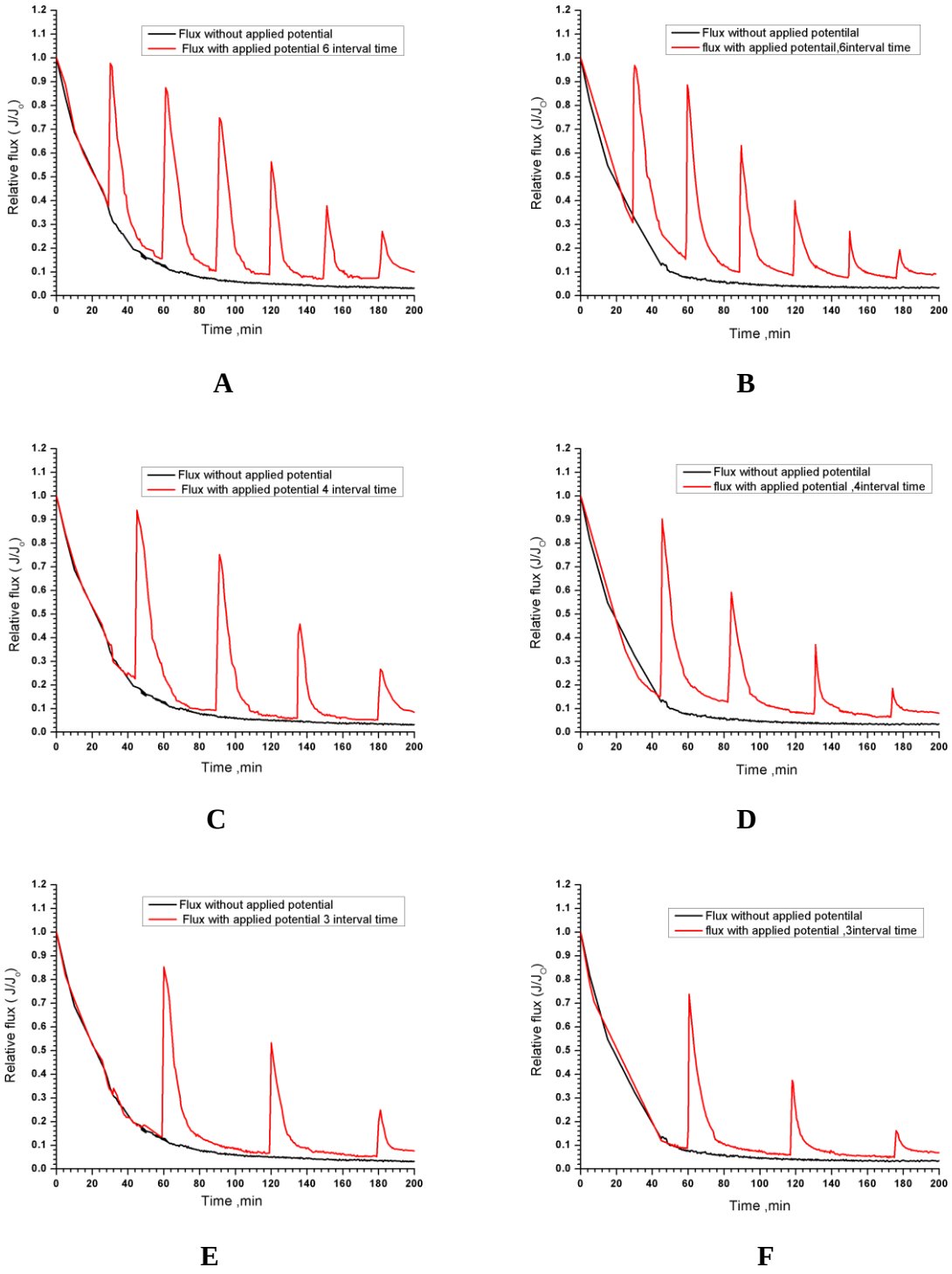

Fig: 7: Relative flux versus filtration time of 8 ppm HA suspension with and without electrolysis using (a) Feed spacer A after 30min filtration intervals (b) Feed spacer B after 30min filtration intervals (c) Feed spacer A after 45 min filtration intervals (d) Feed spacer B after 45 min filtration intervals (e) Feed spacer A after 60min filtration intervals (f) Feed spacer B after 60min filtration intervals.

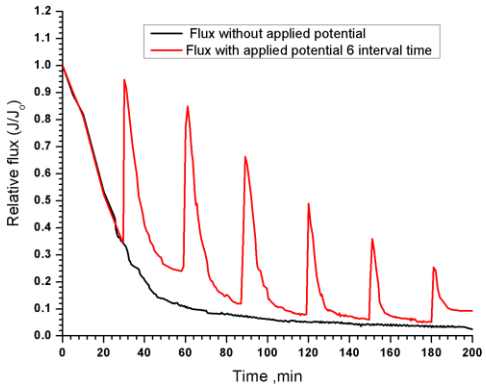

A

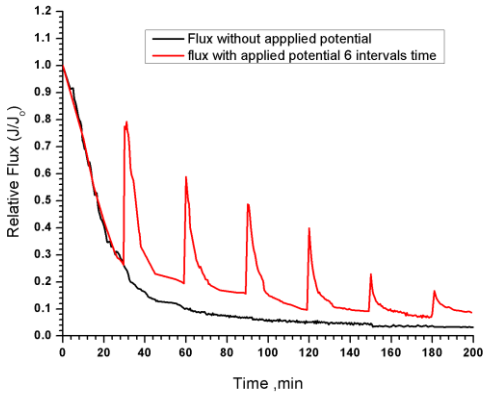

B

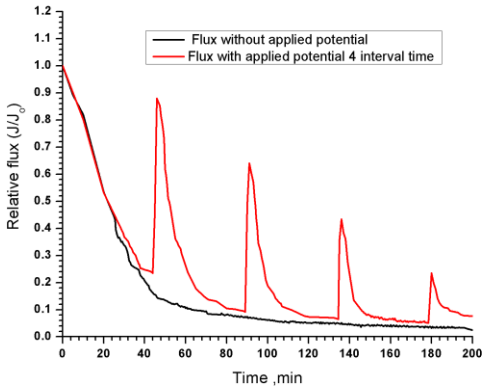

C

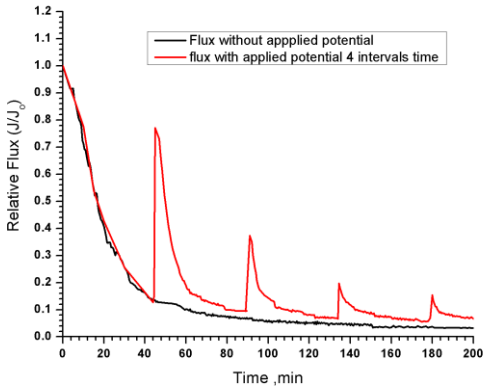

D

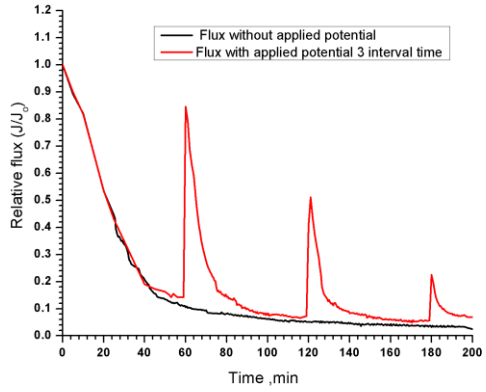

E

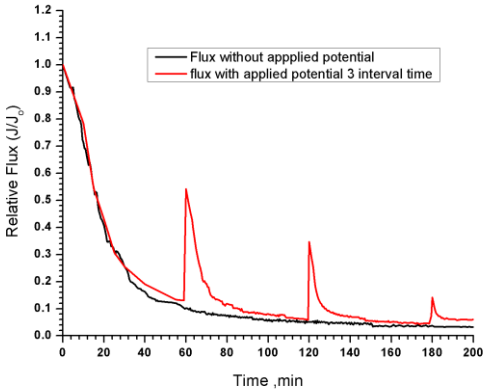

F

Fig: 8: Relative flux versus filtration time filtration of 12 ppm HA suspension with and without electrolysis using (a) Feed spacer A after 30min filtration intervals (b) Feed spacer B after 30min filtration intervals (c) Feed spacer A after 45 min filtration intervals (d) Feed spacer B after 45 min filtration intervals (e) Feed spacer A after 60min filtration intervals (f) Feed spacer B after 60min filtration intervals.

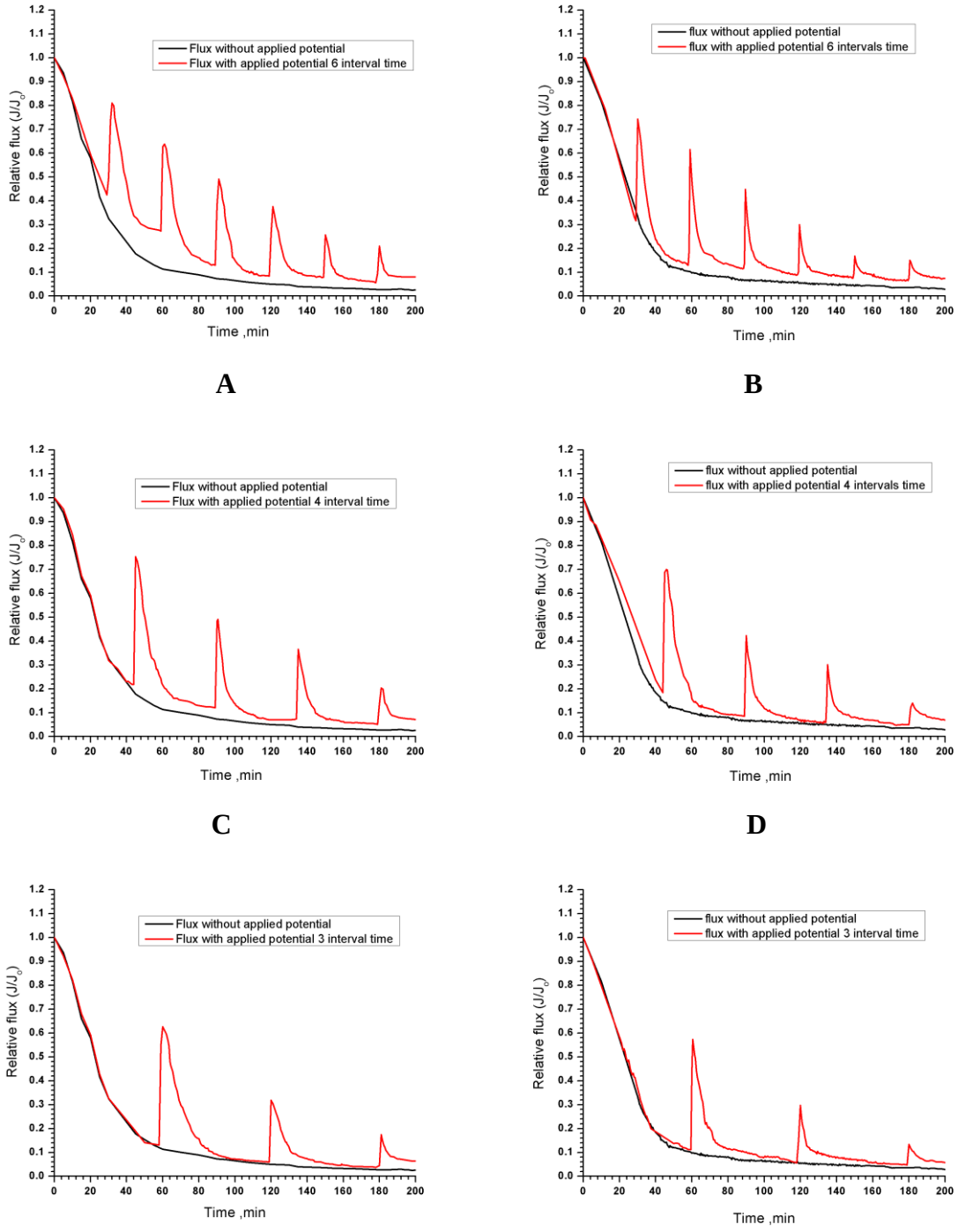

Fig: 9: Relative flux versus filtration time filtration of 16 ppm HA suspension with and without electrolysis using (a) Feed spacer A after 30min filtration intervals (b) Feed spacer B after 30min filtration intervals (c) Feed spacer A after 45 min filtration intervals (d) Feed spacer B after 45 min filtration intervals (e) Feed spacer A after 60min filtration intervals (f) Feed spacer B after 60min filtration intervals.

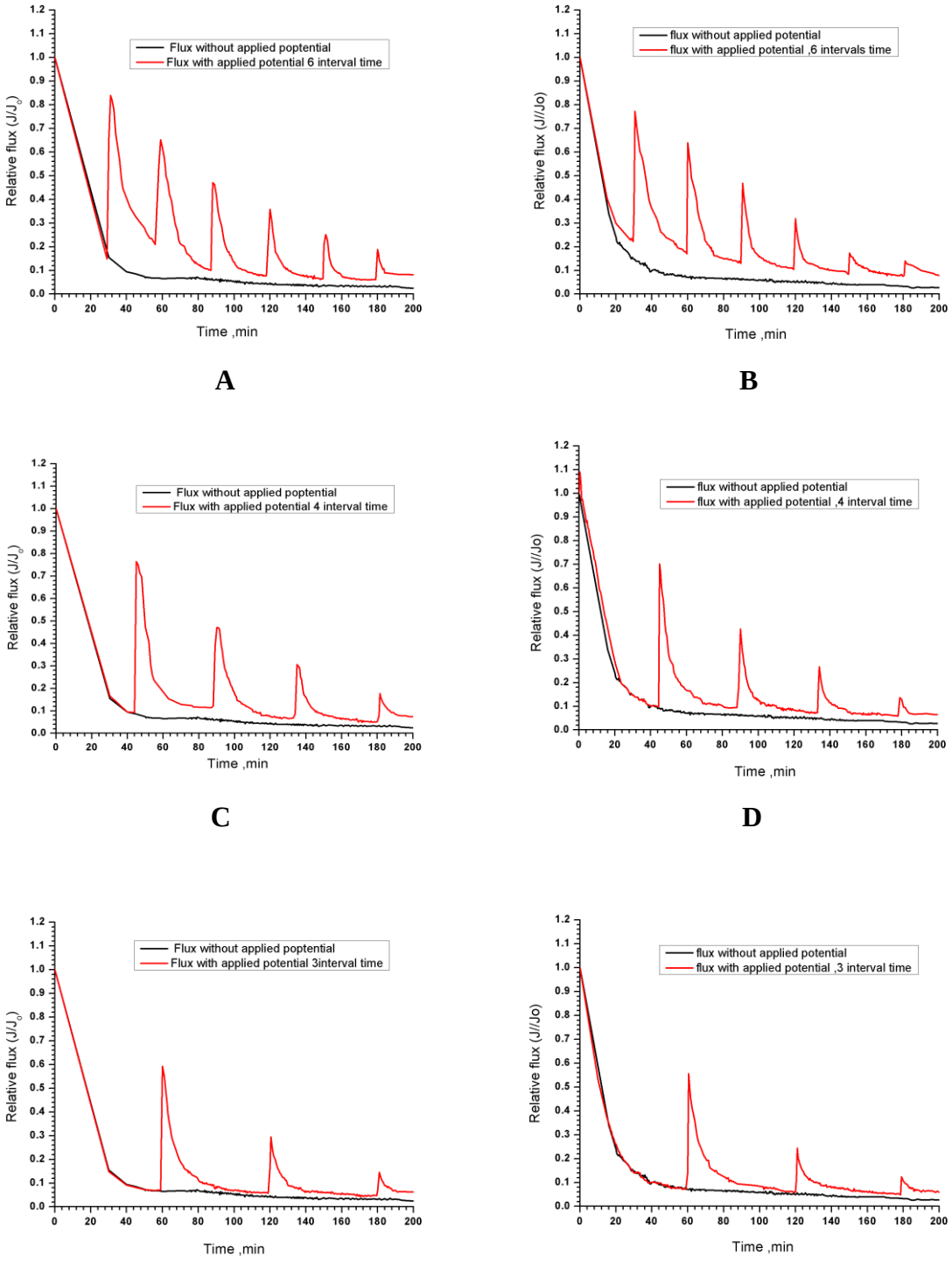

Fig: 10: Relative flux versus filtration time duration of HA suspension with and without electrolysis using (a) Feed spacer A after 30min filtration intervals (b) Feed spacer B after 30min filtration intervals (c) Feed spacer A after 45 min filtration intervals (d) Feed spacer B after 45 min filtration intervals (e) Feed spacer A after 60min filtration intervals (f) Feed spacer B after 60min filtration intervals.

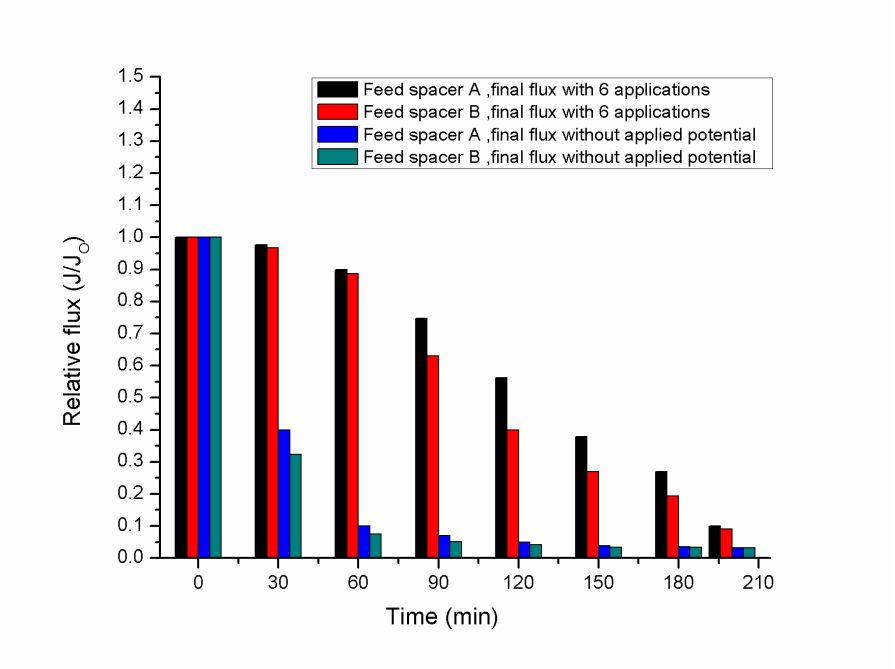
Feed spacer A ,final flux with 6 applications
Feed spacer B ,final flux with 6 applications
Feed spacer A ,final flux without applied potential
Feed spacer B ,final flux without applied potential
Relative flux (J/J$_O$)
Time (min)
0.0
0.1
0.2
0.3
0.4
0.5
0.6
0.7
0.8
0.9
1.0
1.1
1.2
1.3
1.4
1.5
0
30
60
90
120
150
180
210

A

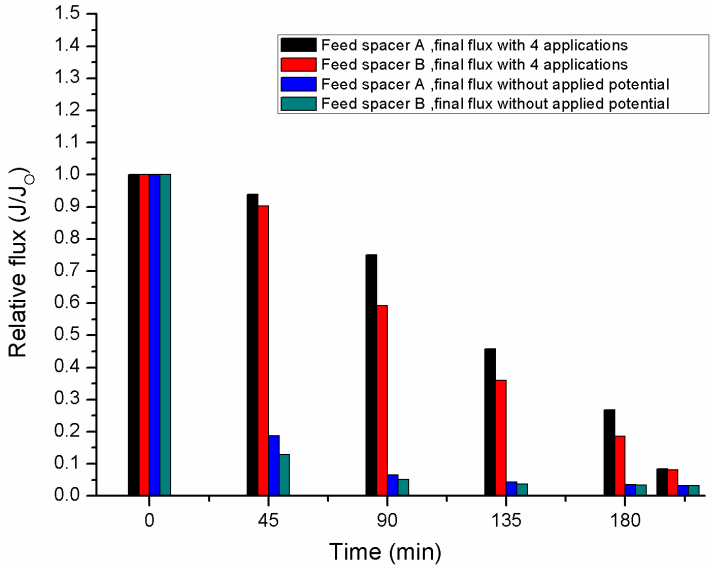
Feed spacer A ,final flux with 4 applications
Feed spacer B ,final flux with 4 applications
Feed spacer A ,final flux without applied potential
Feed spacer B ,final flux without applied potential
Relative flux (J/J$_O$)
Time (min)
0.0
0.1
0.2
0.3
0.4
0.5
0.6
0.7
0.8
0.9
1.0
1.1
1.2
1.3
1.4
1.5
0
45
90
135
180

B

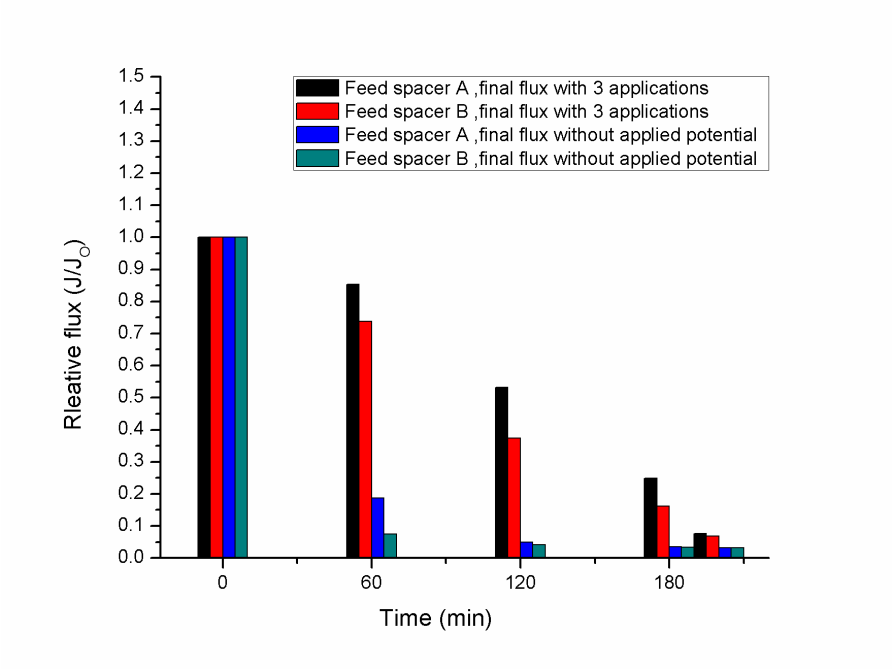

C

Fig: 11: A comparison between relative flux values of HA with concentration 8ppm gained after each interval for using both feed spacer A and feed spacer B (a) 30min filtration interval (b) 45min filtration interval (c) 60min filtration interval

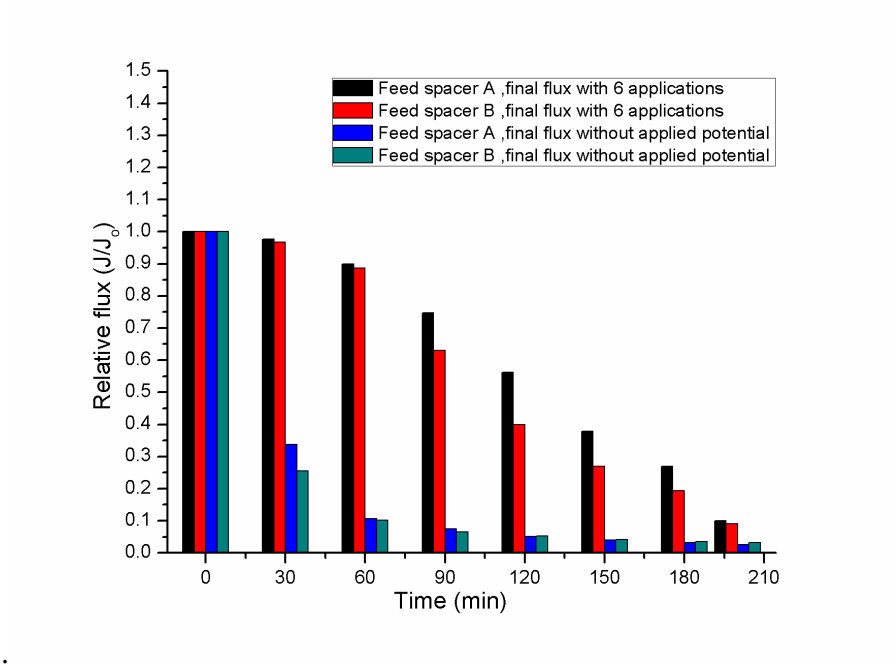

.

A

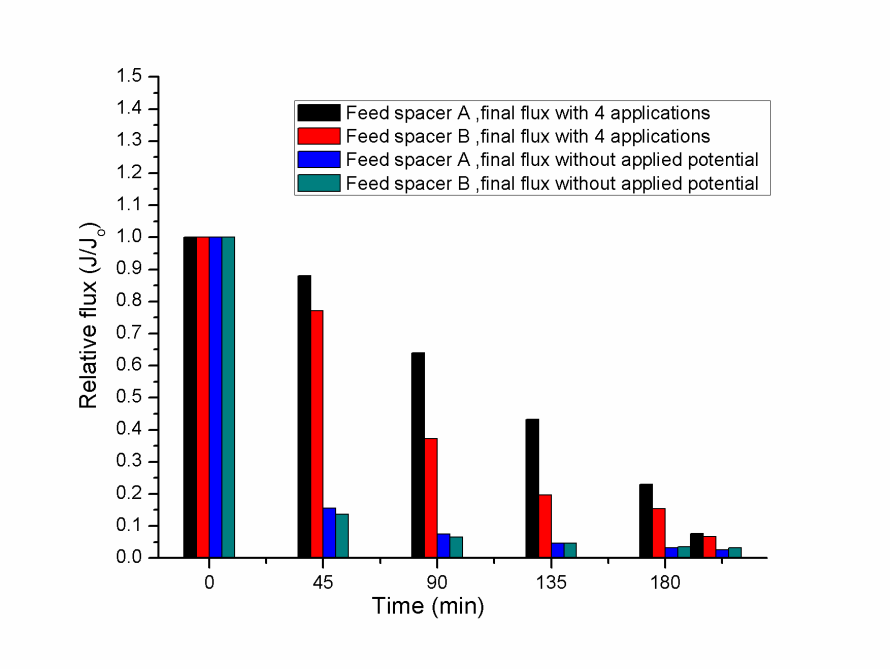

B

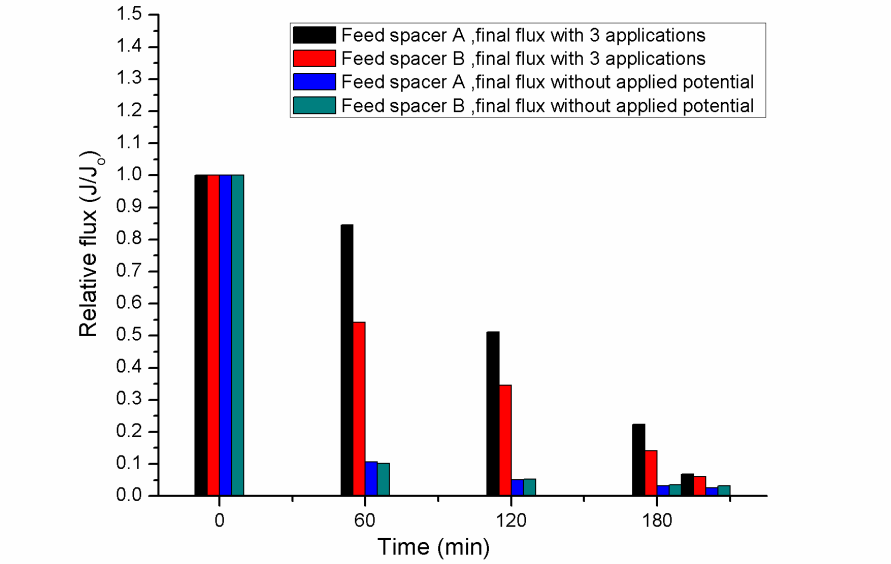

C

Fig: 12: A comparison between relative flux values of HA with concentration 12 ppm gained after each interval for using both feed spacer A and feed spacer B (a) 30min filtration interval (b) 45min filtration interval (c) 60min filtration interval

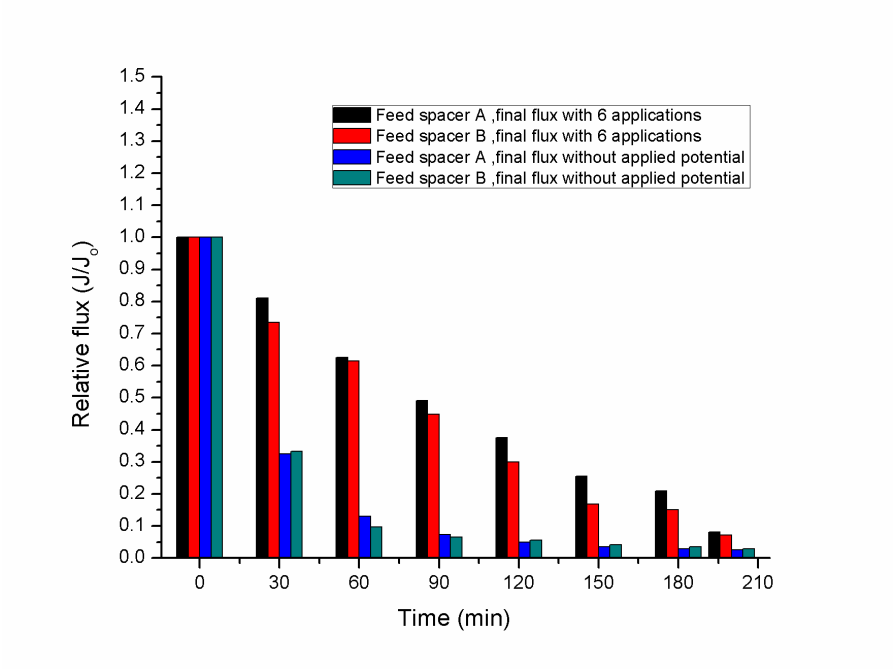
Feed spacer A ,final flux with 6 applications
Feed spacer B ,final flux with 6 applications
Feed spacer A ,final flux without applied potential
Feed spacer B ,final flux without applied potential
Relative flux (J/J$_o$)
Time (min)
0
30
60
90
120
150
180
210

A

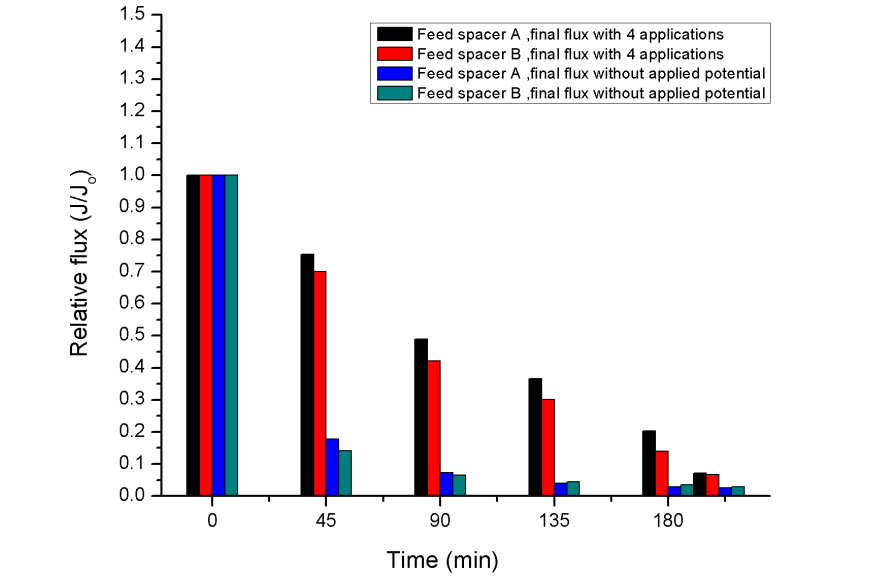
Feed spacer A ,final flux with 4 applications
Feed spacer B ,final flux with 4 applications
Feed spacer A ,final flux without applied potential
Feed spacer B ,final flux without applied potential
Relative flux (J/J$_o$)
Time (min)
0
45
90
135
180

B

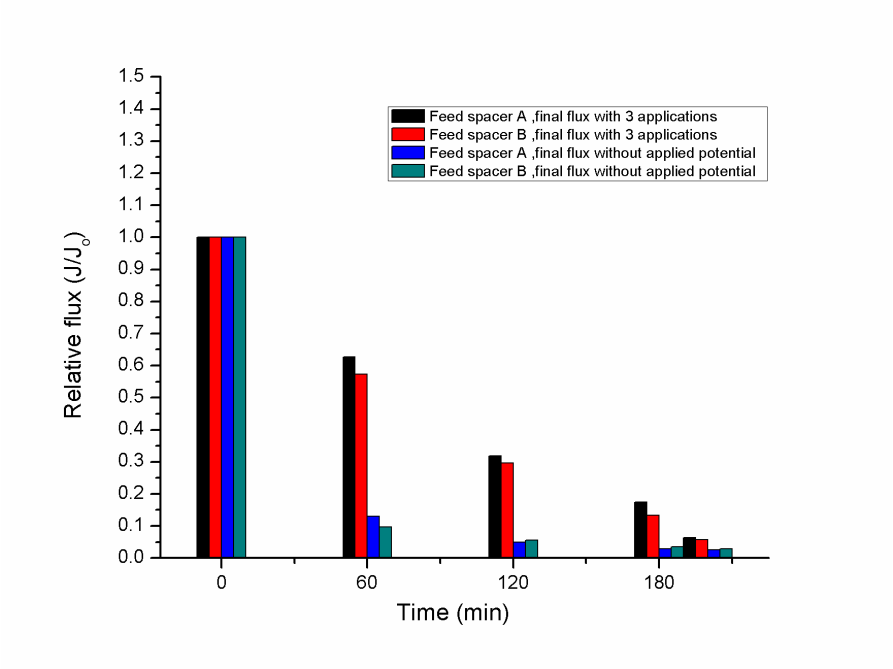

C

Fig: 13: A comparison between relative flux values of HA with concentration 16 ppm gained after each interval for using both feed spacer A and feed spacer B (a) 30min filtration interval (b) 45min filtration interval (c) 60min filtration interval.

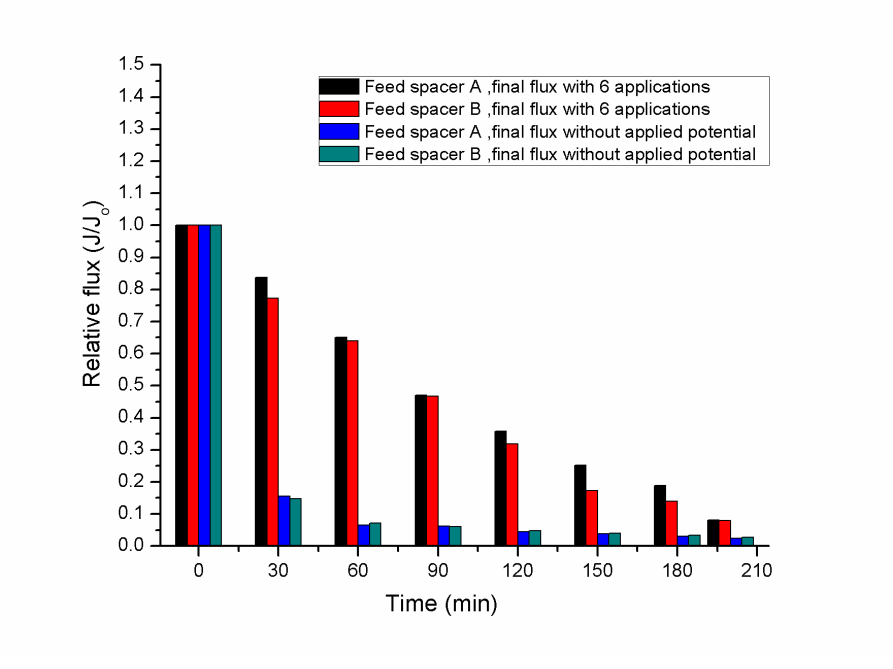

A

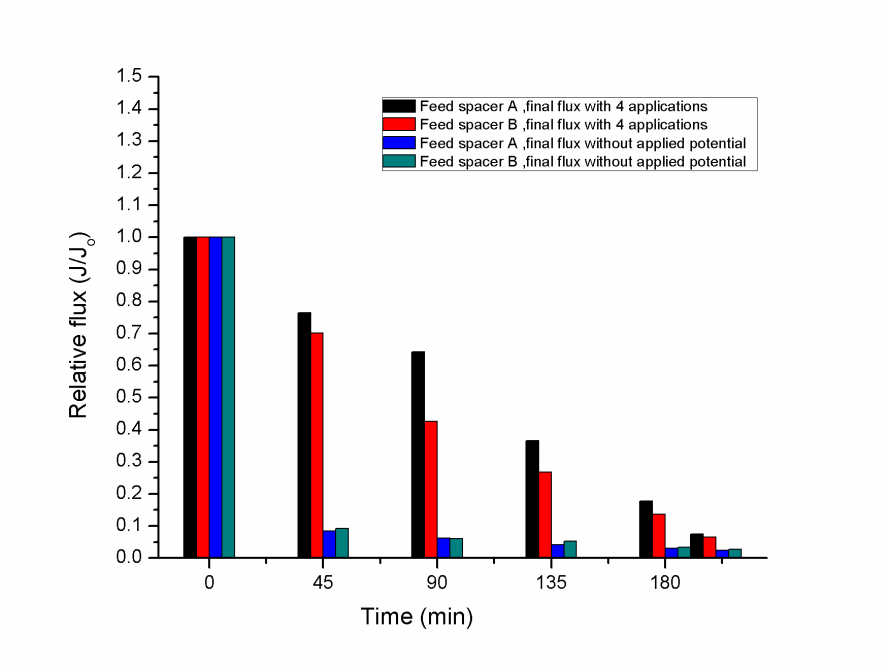

B

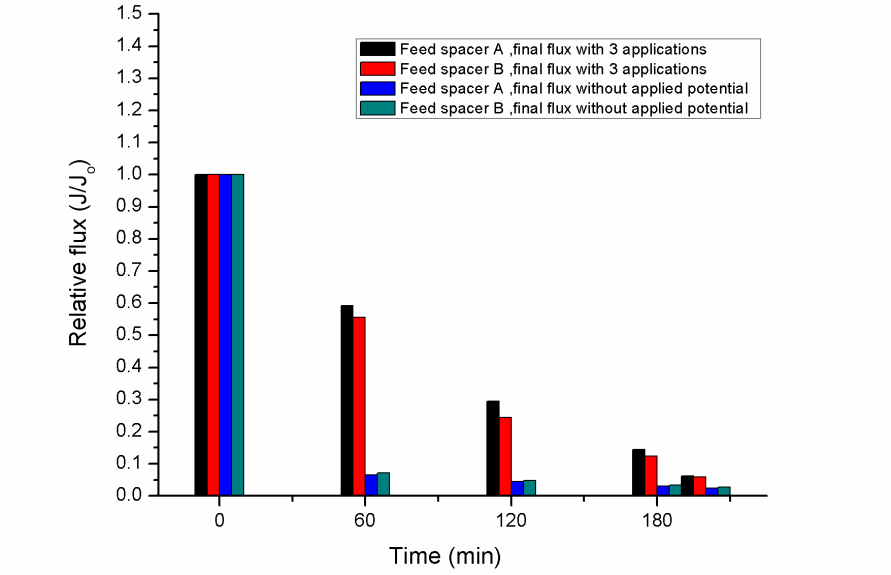

C

Fig: 14: A comparison between relative flux values of HA with concentration 20 ppm gained after each interval for using both feed spacer A and feed spacer B (a) 30min filtration interval (b) 45min filtration interval (c) 60min filtration interval.

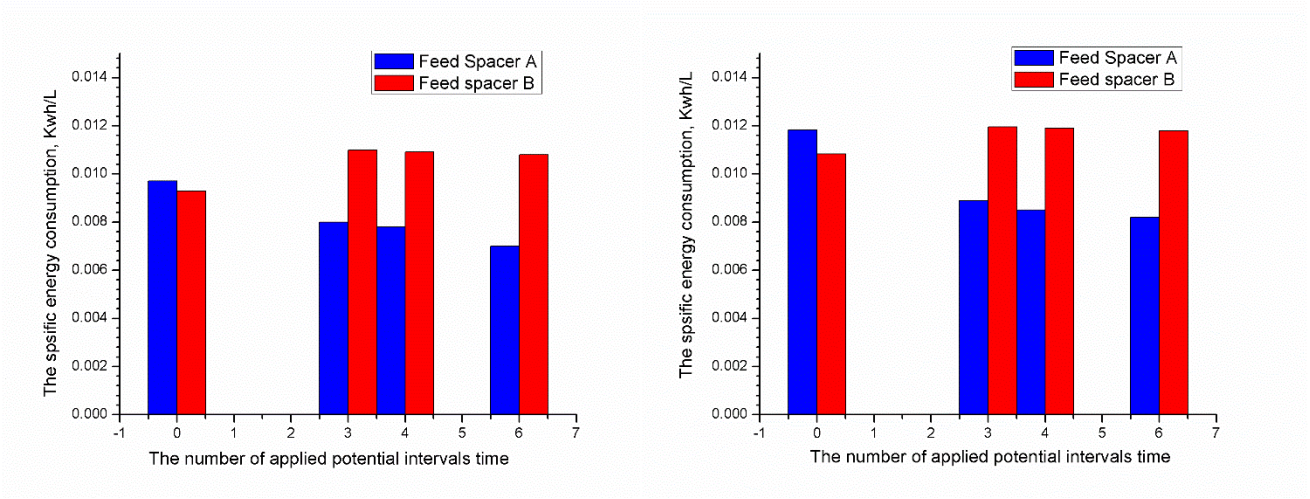

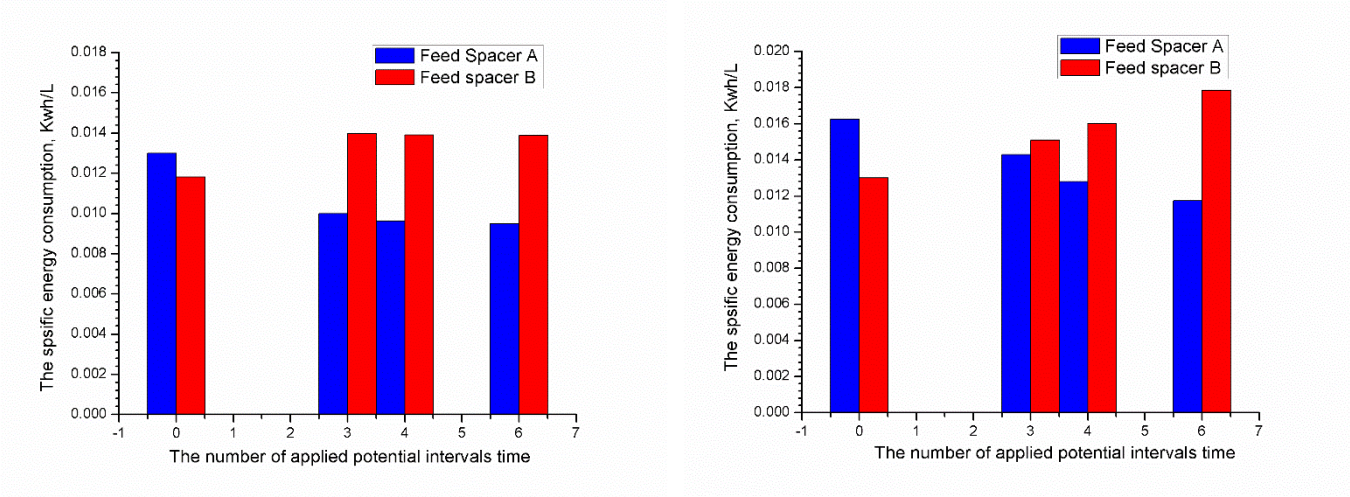

Fig 15: The specific consumption energy for (a) 8 ppm, (b) 12ppm, (c) 16ppm and (d) 20 ppm humic acid concentration during 6, 4, 3 and zero intervals applied potential time for Feed Spacer A and B.

.

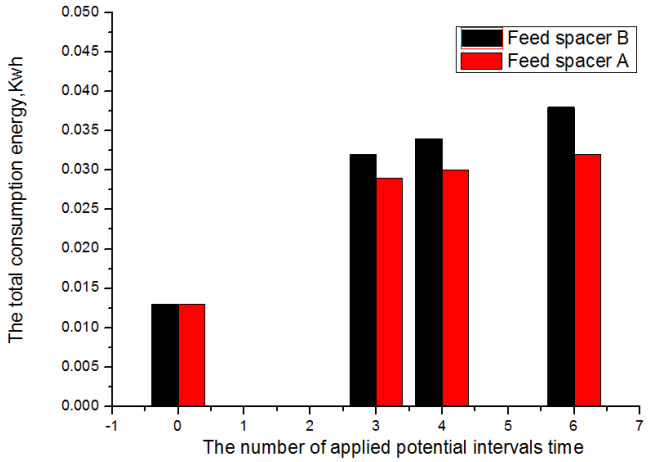

Fig: 15: The effect of feed spacer configuration on the total energy consumption.

List of tables

Table-1: Water quality Parameter

	8 ppm	12 ppm	16 ppm	20 ppm
PH	7 ± 0.5			
Zp mV	-27.7	- 30.3	-32.9	-40.3

Table-2: Characteristics of experimental membrane and feed spacer

Parameter	GVWP
Normal pore size µm	0.22
Material	PVDF
Surface prosperity	Hydrophilic
Pure water flux (L/m2.hr)	4177.05
Membrane surface zeta potential mV	-22
Feed Spacer A aperture	2mm
Feed Spacer B aperture	3mm